Journal of Photochemistry & Photobiology, B: Biology 261 (2024) 113050

Contents lists available at ScienceDirect

Journal of Photochemistry & Photobiology, B: Biology

journal homepage: www.elsevier.com/locate/jphotobiol

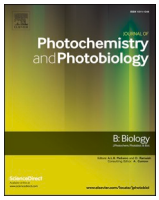

Novel synthetic UV screen compounds inspired in mycosporine-like amino acids (MAAs): Antioxidant capacity, photoprotective properties and toxicity

Félix L. Figueroa [a,*], Pablo Castro-Varela [a,b], Julia Vega [a], Raúl Losantos [c], Beatriz Peñín [c], Leonardo López-Cóndor [c], María Jesús Pacheco [d], Sofía Latorre Redoli [e], Manuel Marí-Beffa [a,d,e], Roberto Abdala-Díaz [a], Diego Sampedro [c]

[a] Universidad de Málaga, Instituto Andaluz de Biotecnología y Desarrollo Azul (IBYDA), Centro Experimental Grice Hutchinson, Lomas de San Julián, 2, 29004 Málaga, Spain
[b] Departamento de Botánica, Facultad de Ciencias Naturales y Oceanográficas, Universidad de Concepción, Chile
[c] Departamento de Química, Instituto de Investigación en Química (IQUR), Universidad de La Rioja, Madre de Dios, 53, 26006 Logroño, La Rioja, Spain
[d] Instituto de Investigación Biomédica de Málaga y Plataforma en Nanomedicina (IBIMA Plataforma BIONAND), Málaga, Spain
[e] Departamento de Biología Celular, Genética y Fisiología, Facultad de Ciencias, Universidad de Málaga, Málaga, Spain

ARTICLE INFO

Keywords:
Cytotoxicity
Mycosporine-like amino acids
Synthesis
UV-screen
Zebrafish acute toxicity assay

ABSTRACT

The combination of environmental stress on the ozone layer, climate change and a greater sun exposure due to outdoor habits has led to an increase in skin cancer cases and other health issues related with UV radiation. Researchers are searching for new alternative UV filters that could protect our skin from the deleterious effects of UV radiation while also presenting low toxicity and biodegradable character (unlike the UV filters currently available in the market). In this work, two compounds inspired in the natural oxo-mycosporine-like amino acids (MAAs) have been synthesized and their antioxidant and photoprotective properties, as well as their *in vitro* and *in vivo* toxicity effects were evaluated. Both compounds featured a strong UV-B absorption together with a high antioxidant capacity, close to 50 μmol TE g^{-1} DW in the ABTS assay. Compound **1** presented an absorption peak at 285–300 nm, whereas compound **2** showed a wider band with a peak around 295–305 nm and two shoulders at 318 and 342 nm. The addition of 5 % of compound **2** to galenic formulas increased the photoprotection, reaching SPF values of 4. Both compounds were stable under UV radiation exposure. Regarding toxicity, the synthetic compounds did not show cytotoxic activity against healthy human cell lines or significant toxicity over zebrafish embryos. Compound **1** showed a complete lack of toxicity over zebrafish, although compound **2** showed slight, not-significant effects on viability, hatching, pericardial stability or body axis formation over 5 mg mL^{-1}. Moreover, compound **1** presented relatively antitumoral activities against HCT-116 cells (selective index:1.49). The relevant antioxidant and photoprotective ability together with the great advantage provided by the reduced toxicity to health cells or zebrafish embryos, make these compounds promising candidates to be exploited as functional ingredients with specific applications in the biotechnological or pharma sector.

1. Introduction

During the last century, anthropogenic impacts have led to an increase of the UV-B radiation that reaches the Earth's surface mainly due to the emission of chlorofluorocarbons (CFCs) and other chemicals that degrade the ozone layer. Nowadays, the ozone layer hole is recovering thanks to the adoption of the Montreal protocol in 1989, that regulate the production and emissions of CFCs and other ozone depleting chemicals (ODCs) [1–3]. However, climate change is further altering atmospheric circulation, and this contributes to less cloudiness and aerosols in terrestrial areas. These changes may also provoke an increase in the UV-B radiation that reaches certain areas of the world. For instance, it is expected that in southern-eastern Asia the UVI (Ultraviolet index) could increase 20–40 %, whereas in central Europe and the eastern part of North America a 5–10 % increase is expected [1]. These effects, together with the current lifestyle, characterized by a high sun exposure due to recreational or working activities outdoor, have contributed to the increase of skin and eyes problems in the worldwide

* Corresponding author.
E-mail address: felix_lopez@uma.es (F.L. Figueroa).

https://doi.org/10.1016/j.jphotobiol.2024.113050
Received 22 April 2024; Received in revised form 14 October 2024; Accepted 30 October 2024
Available online 2 November 2024

population caused by an excess of UV radiation exposure (*e.g.* sunburn, cataracts, immunosuppression, premature photo-aging of the skin, photocarcinogenesis) [4–8].

The use of sunscreens has been proved to prevent the damages caused to our health by UV radiation [9]. These types of creams contain UV filters that either absorb or dissipate the UV rays, preventing them from penetrating into the skin. These filters are generally divided into synthetic (also known as chemical or organic), with the capacity to absorb the UV radiation, and mineral filters (also known as physical or inorganic), that can also reflect, or scatter it [8]. Recently, the environmental and human health safety of certain UV filters (mainly synthetic ones) have been questioned. A variety of organic UV filters have been observed in aquatic organisms (many of them with commercial uses like mussels, clams, crabs, squids or fishes), causing several negative effects (*e.g.* coral bleaching, phytoplankton growth reduction, larvae malformations or hormone disorders) [10–17]. In addition, certain synthetic UV filters can pose a risk for human health, especially those related to endocrine disruptions, photoallergies or oxidative stress [18,19].

In the last years, the European Commission (EC) [20] and the Food and Drugs Administration (FDA) [21] have published restrictions and prohibitions regarding the use of certain UV filters. In 2022, the EC restricted the use of oxybenzone and octocrylene concerning their potential capacity to cause endocrine disruptions [22]. On the other hand, in 2021 the FDA established three different categories of UV filters, namely "Generally Recognized as Safe and Effective" (GRASE), not GRASE due to safety issues, or not GRASE due to lack of safety information. The mineral UV filters, titanium dioxide and zinc oxide, are the only ones categorized as GRASE, whereas two synthetic UV filters (PABA and trolamine salicylate) are categorized as not GRASE due to safety issues, and they are no longer used in US sunscreens. In addition, some areas with valuable marine ecosystem such as Hawaii, Palau or some Caribbean islands have banned the use of sunscreens with certain UV filters, such as oxybenzone or octinoxate, to protect marine habitat [23].

In this scenario, there is a need to search for and develop new UV filters that can cope with the increasing dose of UV radiation that reaches our skin and show a low toxicity profile and a biodegradable character. As a source of inspiration, nature can provide new designs to obtain molecules with the ability to absorb the UV radiation. The extraction and purification of molecules from natural resources can be very expensive and time-consuming. On top of this, the purification of large quantities of molecules that can be used commercially entails having access to huge amounts of biomass, something that is often the bottleneck for the industrial application of any new natural compound. Therefore, scalable, cheap, and affordable synthesis of molecules with suitable properties inspired by nature can be a feasible alternative.

Mycosporine-like amino acids (MAAS) are photoprotective molecules that are mainly found in organisms exposed to high solar radiation such as red intertidal algae, cyanobacteria, or marine lichens. They are a diverse group of nitrogenous compounds, with low molecular weight (< 400 Da), water-soluble character and the ability to absorb UV radiation. There are more than 30 compounds in the MAAs family. All of them share the same central structure, a cyclohexanone or cyclohexenimine ring, responsible for UV absorption. The different types of MAAs vary according to their nitrogen substituent in the chromophore, which determines their specific absorption spectra, ranging from 310 to 360 nm [24–29]. These natural compounds are considered promising candidates as natural UV filters in sunscreens. In addition to the photoprotective properties of these molecules, other beneficial properties for the skin have been described, such as antioxidant capacity, anti-aging potential and immune-modulatory properties [30–36]. However, there are currently few MAA-based products available on the market. Red algae extracts enriched in MAAs and with antioxidant and anti-aging effects can be found and marketed as active ingredients for cosmetic products (*e.g.* Helioguard™365, Helionori® or Ronacare®). Regarding sunscreens, only the French company Laboratoires Biarritz markets a sunscreen named ALGA MARIS® that contains *Gelidium corneum* extract (Alga-Gorria®) enriched in trace elements and antioxidants. The commercial use of these compounds has been hampered by their complex process of isolation and purification from natural sources.

Recently, Losantos et al. [37] developed a new family of molecules based on the core of natural MAAs. These MAA analogues can be synthesized easily and with good yields in multigram scale. The wide range of substitutions that can be incorporated into the basic core allows for adjustable physical properties, making it possible to cover the entire UV radiation spectrum by combining several compounds. Depending on the specific substitution, these compounds can relax in the excited state by dissipating the absorbed light energy through different processes. This can occur by following the same deactivation mechanism as natural MAAs (through the out-of-plane movement of the substituents in the core) or through a different mechanism involving an isomerization pathway as the primary deactivation channel [38,39]. Regardless the mechanism of energy dissipation, the synthetic MAAs analogues feature an impressive photostability. As in the case of the natural counterparts, both cyclohexenimine and cyclohexenone cores provide photoprotection. In order to explore the potential industrial use of these compounds, we will focus this work on the cyclohexenone derivatives as they can be easily prepared on a large scale. Thus, in this work we assessed some properties relevant for the practical use of two analogues of the cyclohexanone family of MAAs. The chosen compounds **1** and **2** were selected for their easy and scalable synthesis and promising features revealed in previous reports.

To carry out safety assessments and understand the photoprotective capabilities of these derivatives in sunscreens, we have prepared and studied two compounds inspired by natural oxo-MAAs. Compounds **1** and **2** have been prepared and characterized by their antioxidant capacity, photoprotective properties, and cytotoxicity effects at two levels: i) *in vitro* (on human healthy cells and human carcinoma cells) and ii) *in vivo* (on zebrafish larvae).

2. Material and Methods

2.1. Synthesis of Compounds

Compounds **1** and **2** (Fig. 1) were prepared by condensation of dimedone or 1,3-cyclohexanedione with ethanolamine or diethanolamine in refluxing toluene using a Dean-Stark condenser and a catalytic amount of *p*-toluenesulphonic acid. Both compounds were purified by precipitation using diethyl ether as solvent after rotatory evaporation of toluene. They were finally obtained as pure orange solids with quantitative yields. All reagents were obtained from Merck with synthesis grade. The 1,3-cyclohexanedione was of 97 % purity. Ethanolamine, diethanolamine and *p*-toluenesulphonic acid monohydrate were used with a 98 % purity. All chemicals were used as received without further purification.

2.1.1. Analysis Data

Compound **1 (3-((2-hydroxyethyl)amino)-5,5-dimethylcyclohex-2-en-1-one)**:

HRMS ESI+ (*m/z*) calcd. For $C_{10}H_{18}NO_2$ $[M+H]^+$: 184.1332, found: 184.1339. Err.: 4.0 ppm.

^{1}H NMR (300 MHz, MeOD) δ (ppm): 1.08 (s, 6H), 2.18 (s, 2H), 2.33 (s, 2H), 3.27 (t, $J = 5.7$ Hz, 2H), 3.72 (t, $J = 5.7$ Hz, 2H), 5.14 (s, 1H).

^{13}C NMR (75 MHz, MeOD) δ (ppm): 28.3, 33.6, 43.7, 46.2, 50.5, 60.3, 94.3 (C2), 168.5, 198.9.

Compound **2 (3-(bis(2-hydroxyethyl)amino)cyclohex-2-en-1-one)**:

HRMS ESI+ (*m/z*) calcd. For $C_{10}H_{18}NO_3$ $[M+H]^+$: 200.1281, found: 200.1288. Err.: 3.6 ppm.

^{1}H NMR (300 MHz, MeOD) δ (ppm): 1.92–2.01 (m, 2H), 2.22–2.29 (m, 2H), 2.62–2.71 (m, 2H), 3.57–3.61 (m, 4H), 3.73–3.76 (m, 4H), 5.25 (s, 1H).

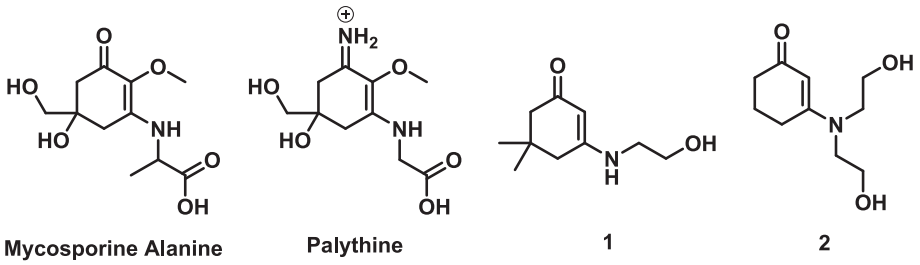

Fig. 1. Chemical structures of natural MAAs: mycosporine alanine and palythine together with the synthetic compounds 1 and 2 studied in this paper.

^{13}C NMR (75 MHz, MeOD) δ (ppm): 23.1, 28.0, 35.8, 54.1, 54.3, 60.7, 60.8, 98.4, 170.3, 199.3.

2.1.2. Computational Details

The geometries were optimized under the Density Functional Theory (DFT) framework using B3LYP/6–31 + G** [40,41]. Solvation effect was computed using water as an implicit solvent within the IEFPCM scheme [42]. Absorption spectra were calculated using Time-Dependent (TD) DFT [43] under equilibrium conditions for the solvent considering 10 transitions to ensure consistency. The natural transition orbitals (NTO) [44] were computed for transitions 1 and 2, *i.e.* S_1 and S_2. All calculations were done using the Gaussian 16C.01 package [45].

2.2. Antioxidant Capacity

Antioxidant capacity was measured using two different methodologies based on free radical scavenging capacity, the ABTS and the DPHH assays. To perform these assays, compounds **1** and **2** were dissolved in distilled H_2O at a concentration of 4 mg mL^{-1}. For both methods, a standard solution of Trolox (6-hydroxy-2,5,7,8-tetramethylchroman-2-carboxylic acid) was used as reference and the results were expressed as μmol TE (Trolox equivalent) g^{-1} DW.

The ABTS (2,2′-azino-bis(3-ethylbenzothiazoline-6-sulfonic acid)) assay was performed as described Re et al. [46] with some modifications. The radical cation ABTS$^{+\bullet}$ was generated by mixing 7 mM of ABTS (2,2′-azino-bis(3-ethylbenzothiazoline-6-sulfonic acid) and 2.45 mM of $K_2S_2O_8$ in phosphate buffer (0.1 M, pH 7). This mixture was stored at room temperature for 12-16 h to ensure the complete formation of the radical. For the assay, ABTS$^{+\bullet}$ solution was diluted with phosphate buffer until absorbance at 727 nm was about 0.75 ± 0.05. 50 μL of the samples were mixed with 950 μL of the diluted ABTS$^{+\bullet}$, incubated during 8 min at room temperature and darkness and measured spectrophotometrically (UV-2600, Shimadzu, Duisburg, Germany) at 727 nm.

The DPPH (2,2-difenil-1-picrilhidracilo) assay was performed according to Brand-Williams et al. [47] with some modifications. For the reaction, 800 μL of the DPPH (2,2-diphenyl-1-picrylhydrazyl) solution (0.06 mM of DPPH in methanol 80 %) was mixed with 200 μL of the samples. After 15 min of incubation at room temperature and darkness, absorbance was measured at 517 nm.

2.3. Photoprotection Factors

For the determination of the different photoprotection factors, compounds **1** and **2** were added to a base cream as powder in two different percentages (2.5 and 5 %). The synthetic molecules and the base cream were manually mixed until a homogenous mixture was obtained.

The methodology used to obtain the photoprotection factors were based on de la Coba et al., ISO 24443 and Pissavini et al. [31,48,49]. To do this, 32.5 mg of the different creams were spread on polymethyl methacrylate (PMMA) plates with a 25 mm × 25 mm surface and 6 μm roughness (Schonberg, Germany). The creams were spread with the fingertip of a glove (previously saturated with the cream) for no more than a minute. After 15 min of incubation in darkness and at room temperature, transmittance through the plates were measured using the spectrophotometer with an integrated sphere (ISR-2600Plus, Shimadzu, Duisburg, Germany). Transmittance (T) values were converted to absorbance (Abs) values as Abs = log (T). Each cream was spread on three plates and each plate was measured twice.

The solar protection factor (SPF) was calculated using the erythematic action spectrum [48,50]. For the UVA protection factor (UVAPF), the persistent pigment darkening action spectrum [49,51] was used. Other biological effective protection factors (BEPFs) were calculated using other action spectra related with the UV radiation [31] related to UVB exposure as photocarcinogenesis [52], immunosuppression [53] and related to UVA exposure as elastosis [54], singlet oxygen formation [55] and photoaging [56]. The following formula was used in all cases:

$$PPFs = \frac{\int_{\lambda=290}^{\lambda=400} Act.Sp(\lambda)\ x\ E(\lambda)\ x\ d(\lambda)}{\int_{\lambda=290}^{\lambda=400} Act.Sp(\lambda)\ x\ E(\lambda)\ x\ 10^{-Abs(\lambda)}\ x\ d(\lambda)}$$

where, PPFs = Photoprotection Factors, Act.*sp.* (λ) = action spectra (0–1); E (λ) = spectral irradiance of a sunny midday in summer in Malaga (W m^{-2}); d (λ) = wavelength step (1 nm); Abs (λ) = Absorbance values (0–1).

The critical lambda (λ_c) was also calculated as the wavelength (from 290 to 400 nm) at which each cream absorbed 90 % of the radiation.

Creams were also submitted to photostability tests. For that, PMMA plates with the spread creams were irradiated with an UV lamp during 30 and 60 min. The UV lamp consist in three QPanel340 fluorescent lamps (Q-lab Corporation, Canada) with an intensity of 46.4 W m^{-2} (UVB = 2.8 W m^{-2}; UV-A = 43.4 W m^{-2}). The UV irradiation dose of the lamp was 83.4 and 167.2 kJ m^{-2} for the 30 and 60 min, respectively. The erythemal dose and its equivalation to the minimal erythemal dose (MED) is observed in Table 1. After the irradiation time, transmittance across the plates was determined again as described above.

2.4. Cellular Toxicity Through MTT Assay (In Vitro)

To perform the cytotoxicity analysis, human cell lines were obtained from the American Type Culture Collection (ATCC, USA) and the Bank of cells of Granada University (CIG-UGA, Spain). All the cell lines are maintained and deposited in bank of cells of the Research Support Services (SCAI-UMA) according to the ATCC reference biological procedure for research (www.atcc.org) and Institutional Review Board-approved

Table 1
Irradiation time, erythemal dose and its equivalation to the minimal erythemal dose (MED) of people with phototype II, that correspond to an erythemal dose of 250–400 J m^{-2}.

UV exposure time (min)	Erythemal dose (J m^{-2})	Equivalation to MED
30	484.48	1.2–1.9
60	970.82	2.4–3.9

protocols at the Malaga University. For this, two healthy human cell lines: (1) human fibroblasts (CCD-1064sk, CIC-UGA, n° ATCC: CRL-2076), used from passage 11; and (2) human primary epidermal keratinocytes (HEKa, HaCat, ATCC, USA, n° ATCC: PCS 200–011), used from passage 13; and three carcinogenic cell lines: (3) lung cancer (NCI-H-460, ATCC, USA, n° ATCC: HTB-177), used from passage 6; (4) human malignant melanoma (G-361, ATCC, USA, n° ATCC: CRL-1424), used from passage 15; and human colon cancer (HCT-116, ATCC, USA, n° ATCC CCL-247, used from passage 7). No myoplasm contamination was detected in any of the cell lines. 1064sk, and HCT-116 s cell lines were cultured using Dulbecco's modified Eagle's medium (DMEM; Capricorn Scientific). HACAT, H-460 and G-361 were grown in RPMI-1640 medium (BioWhittaker). Both media were supplemented with 10 % fetal bovine serum (Biowest), 1 % penicillin–streptomycin solution (Capricorn Scientific), and 0.5 % of amphotericin B (Biowest). Cells were cultured at 37 °C under subconfluence in an atmosphere-controlled incubator with 5 % CO_2.

The MTT assay were performed as Castro-Varela et al. [57]. Cells were incubated with different concentrations of the synthetic compounds (20 to 0.007 mg mL^{-1}). The incubations were performed in 96-wells microplates for 72 h at 37 °C and with 5 % CO_2. After incubation time, 10 mL of the MTT (3-(4,5-dimethylthiazol-2-yl)-2,5-diphenyltetrazolium bromide) solution (5 mg mL^{-1} in phosphate buffered saline solution) were added to each well. After 4 h of incubation (37 °C and 5 % of CO_2), the yellow tetrazolium salt of the MTT was reduced to insoluble purple formazan crystals by the mitochondrial dehydrogenase of metabolically active cells. Formazan crystals were solubilized by the addition of 150 μL of 0.04 N HCl in 2-propanol and absorbance were measured using a microplate reader (Micro Plate Reader 2001, Whittaker Bioproducts, USA) at 550 nm. Results were expressed as the half maximal effective concentration (EC_{50}; mg mL^{-1}).

The selectivity index determines the cytotoxic selectivity of the tested compounds. It was calculated by the ratio between the EC_{50} of healthy and cancerous cell lines, as indicated in the following formula:

$$SI = \frac{\text{EC50 of Healthy cell}}{\text{EC50 of Cancer cell}}$$

According to Indrayanto et al. [58], a selective compound presents a SI over 3.

2.5. Zebrafish Embryo Toxicity Assay (In Vivo)

The toxicity of both synthetic compounds (**1** and **2**) over zebrafish larvae was studied following a variant of the zebrafish embryo toxicity assay (ZEFT) [59]. This method has been incorporated by many international laboratories (Organization for Economic Co-operation and Development, OECD, Test Guideline No. 236), for lethal and teratogenesis assessment of drugs [60]. The method is considered a good alternative to rodent toxicity assays due to its high sensitivity and predictability after validation under the International Conference on Harmonization (ICH) S5(R3) [61].

In our study, we have used *Danio rerio* embryos from mating between AB wild type adults purchased from the European Zebrafish Resource Center. These adults were raised and cultured at the Center of Experimentation and Animal Behaviour of the University of Malaga and the Institute of Biomedical Research of Malaga and Nanomedicine Platform (IBIMA-BIONAND platform). Husbandry was under the European Directive 2010/63/EU and the Spanish Royal Decree 118/2021. Four hours post-fertilization (hpf) eggs were placed in 96-well microplates (one egg per well) with 300 μL of different concentrations of each synthetic compound diluted in E3 embryo medium [60]. Embryos were incubated at 28 ± 0.1 °C for 3 days. First, the eggs were incubated only once at various concentrations between 1 and 20 mg mL^{-1} of compounds **1** or **2** to determine the most appropriate concentrations. The definitive experiments with the selected concentrations were run at least three times. Incubations in E3 embryo medium were used as negative controls, while a 2 mg mL^{-1} ulvan polysaccharide were used as a positive control [62].

Various anatomical features of each specimen were noted daily from digital images obtained under a Nikon Microphot-FX Fluorescence Microscope (Nikon DS-L1 camera, USA) or directly under a magnifying microscope (Nikon SMZ-445, USA). Viability, chorion lysis, cardiac oedema and hatching are some of the most common features observed. Coagulation or no heartbeat of embryos was used to determine lethal endpoints. Log-linear regression test from viability data was used to estimate the concentration that kills 50 % of the tested embryos (50 % lethal concentration, LC_{50}) [63]. After the experiments, the 120 hpf embryos were euthanized by over-anesthesia.

2.6. Statistical Analysis

To determine the statistical differences between each treatment, a one-way analysis of variance (ANOVA) was performed followed by a Student Newman Keuls (SNK) test. Homogeneity of variance was evaluated using the Cochran test and visual inspection of the residuals. All *in vitro* and chemical analyses were performed using SPSS v.21 (IBM, USA).

Statistical differences between zebrafish data was calculated by a Kruskal-Wallis test followed by a pairwise Mann–Whitney test with Bonferroni correction. Non normality of data was determined by Shapiro-Wilk test. Tests were done using Statgraphics Centurion 19 (Statgraphics Technology, Inc., Virgina, USA).

The suitability of the assays was estimated by measuring the statistical effect size provided by the Z factor:

$$\text{Z factor} = 1 - \frac{3\,(\text{SD(pc)} + \text{SD(nc)}\,)}{|\text{Mean(pc)} - \text{Mean(nc)}\,|}$$

where SD is standard deviation, pc and nc are positive and negative control data, respectively, and I I is absolute values. By this method, $Z > 0.5$ means highly accurate experimental design, $0.5 \geq Z > 0$ means sufficient accuracy and $Z < 0$ inappropriate experimental design. This factor was calculated for each condition tested [64].

3. Results

Compounds **1** and **2** were prepared as previously described and the UV–Vis spectra was recorded in water. A series of TD-DFT calculations were done to characterize the nature of the excitation under UV light irradiation. Both compounds exhibit a possible two-state excitation, presenting two electronic transitions as the most favored ones. These involve a lower energy n-π* transition that is mainly dark ($f \approx 0$) and another bright π-π* transition of higher energy associated. In Fig. 2, the natural transition orbitals (NTO) show the character of the relevant transitions, which are similar for compounds **1** and **2,** in agreement with experimental results. A blueshift was obtained between the calculated spectrum and the experimental one in water, which is mainly due to the selected functional.

Regarding bioactivities, both synthetic compounds showed antioxidant capacity measured through the ABTS and DPPH assay. In neither of the methodologies used, significant differences were observed between the compounds analyzed ($p > 0.05$; Table SM.1). The ABTS method showed much higher values than DPPH (46.8 and 12.7 μmol TE g^{-1} DW, respectively) (Fig. 3). The *Z*-factors in both antioxidant assays are 0.89.

The addition of the synthetic compounds to the base cream increased the ability to absorb the UV radiation. Compound **1** presents the maximum absorption at 285–300 nm, whereas compound **2** showed a wider spectrum with the highest absorbance between 295 and 305 nm and two shoulders at 318 and 342 nm. Increasing the amount of compound added to the creams also increased the UV absorbance capacity (Fig. 4).

Regarding the different photoprotection factors (PPFs) calculated (Table 2), the cream with compound **1** increased its SPF from 1.2 (base

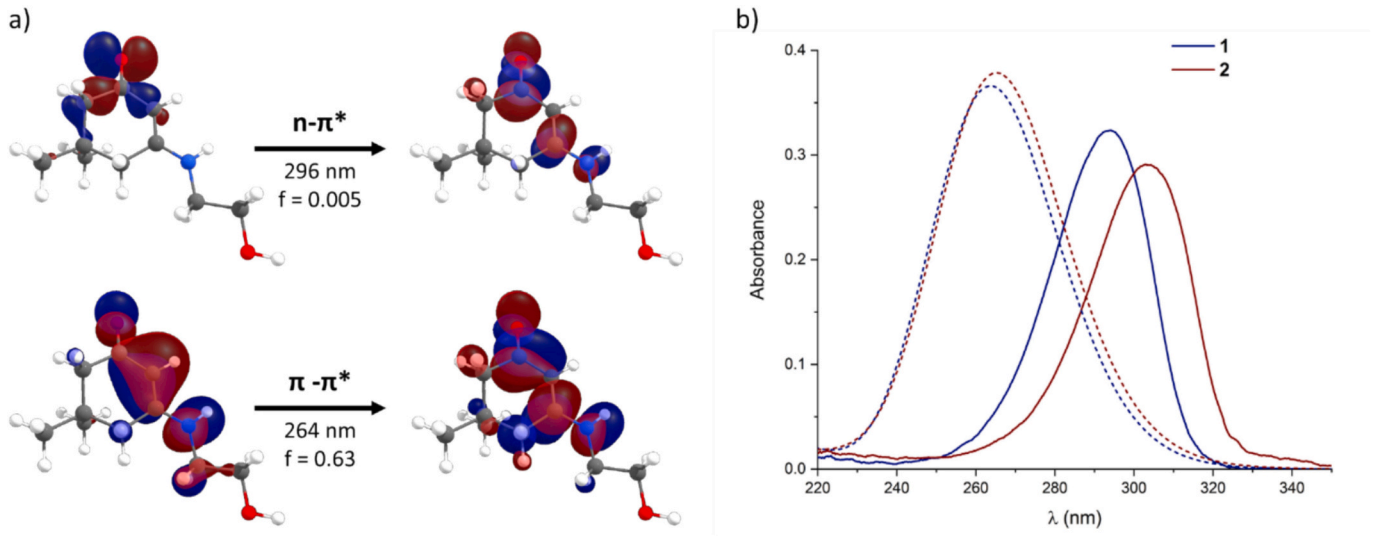

Fig. 2. a) Natural transition orbitals of the two main transitions of compound **1** calculated at B3LYP/6–31 + G**. b) Experimental (solid line) and simulated (dashed line) UV–Vis spectra in water.

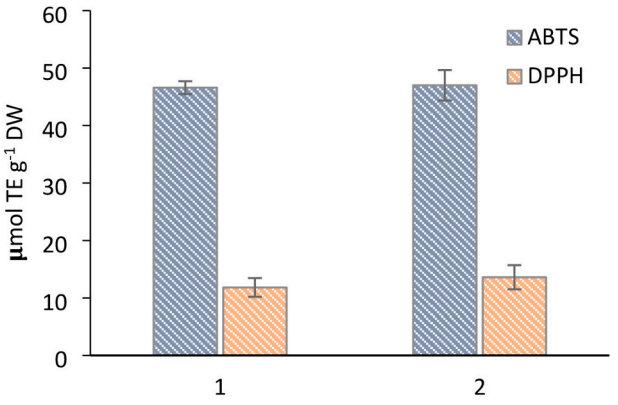

Fig. 3. Antioxidant capacity (µmol Trolox Equivalents (TE) g^{-1} DW) of compounds **1** and **2** measured through ABTS and DPPH methods. Values are expressed as mean ± standard deviation (SD) ($n = 3$). No significant differences were observed between compounds (Student's *t*-test, CI: 95 %, $p > 0.05$).

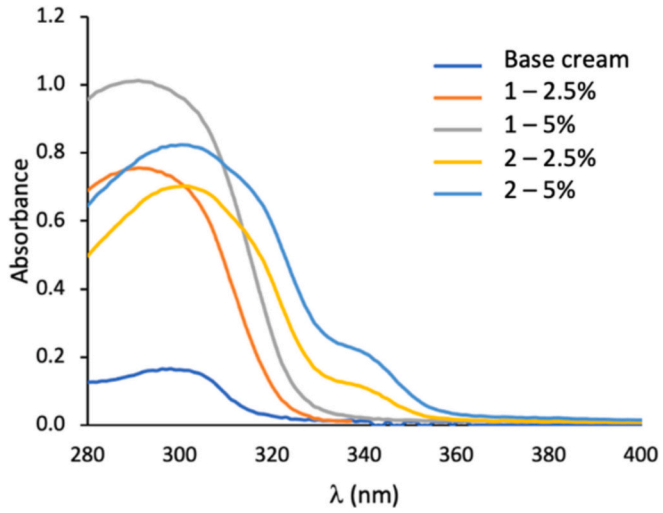

Fig. 4. Absorbance spectrum (290–400 nm) of the base cream and the creams containing 2.5 and 5 % of each synthetic compound (**1** and **2**). Values were expressed as the mean of three replicates ($n = 3$). Absorbance values were divided by the maximum of all creams to obtain values between 0 and 1.

cream) to 2.2 and 3.2 (for the 2.5 and 5 %, respectively). On the other hand, the formula with compound **2** showed higher values, reaching 3.1 and 4 for 2.5 and 5 %, respectively. In UVAPF, only the addition of 5 % of compound **1** showed a significant increase. In this case, the values increased from 1.0 in the base cream to 1.1. In contrast, compound **2** showed a higher increase in UVAPF, showing values of 1.2 and 1.4 after the addition of 2.5 and 5 % of compound **2**. As for the other biological effective protection factors (BEPFs), protection against photocarcinogenesis is the one that showed the highest values, reaching 6.5 and 6.2 when compounds **1** and **2** were added, respectively. Immunosuppression showed similar values to those of SPF. Higher values were observed with compound **2** (reached 5.2) than compound **1** (reach 3.3). Protection against elastosis, the singlet oxygen formation of photoaging (all related with UVA radiation), showed low values similar to those of the UVAPF. The SPF/UVAPF ratio increased when any of the compounds were added to 5 %, showing values of 2.9. The critical lambda (λ_c) was higher with the addition of compound **2** than with compound **1**, reaching values of 331 and 338 with the addition of 2.5 and 5 % of compound **2**, respectively.

The creams with the synthetic compounds were subjected to photostability test. No significant decrease in the PPFs was observed after 30 and 60 min of UV radiation (Figure SM2).

The cytotoxicity of compounds **1** and **2** was determined in different cell lines (both healthy and carcinogenic). As shown in Table 3, both compounds exhibited relatively high and dose-dependent inhibition ratios on cancer cells growth at all concentration levels. The lowest EC_{50} value of compound **1** was on HCT-116 (5.35 ± 2.88 mg mL^{-1}) being higher on H-460 cells (7.76 ± 3.12 mg mL^{-1}) or G-361 (9.48 ± 2.04 mg mL^{-1}; Table 3). Compound **2** also showed the lowest EC_{50} value on HCT-116 cells (11.320 ± 8.36 mg mL^{-1}), while on H-460 EC_{50} it was 11.436 ± 4.0 mg mL^{-1} and on G-361 it was undetected (Table 3). In the case of control healthy cells, only the addition of compounds **1** and **2** on HACAT cells at concentrations higher than 10 mg mL^{-1} for 72 h induced a concentration-dependent decrease in cell survival. In this assay, EC_{50} was 3.06 ± 1.8 mg mL^{-1} and 4.96 ± 3.3 mg mL^{-1} for compounds **1** and **2,** respectively (Table 3). Compound **1** concentrations higher than 20 mg mL^{-1} induced a 95 % decrease of cell survival when compared to untreated cells (Table 3). In general, our results suggested a non-acute cytotoxic effect on cancer and healthy cells, being compound **1** more effective on the cancer cell lines than compound **2**. The highest SI values

Table 2
Solar protection factor (SPF, related to erythema), UVA protection factor (UVAPF, related to persistent pigment darkening-PPD), different biological effective protection factors (BEPFs) against other biological effects of the UV radiation (photocarcinogenesis, immunosuppresion, elastosis, singlet oxygen formation and photoaging), the ratio SPF/UVAPF and critical λ_c. Values are expressed as mean ± standard deviation (SD) (n = 3), except the ratio SPF/UVAPF and λ_c, that was calculated from the average values. Different letters indicate significant differences among the studied creams (ANOVA, SNK, CI: 95 %, $p < 0.05$, table SM.1).

	Base cream	1 (2.5 %)	1 (5 %)	2 (2.5 %)	2 (5 %)
SPF (Erythema)	1.22 ± 0.02^a	2.22 ± 0.09^b	3.17 ± 0.27^c	3.08 ± 0.22^c	3.99 ± 0.72^d
UVAPF (PPD)	1.03 ± 0.00^a	1.03 ± 0.00^a	1.08 ± 0.02^b	1.20 ± 0.02^c	1.35 ± 0.04^d
Photocarcinogenesis	1.40 ± 0.04^a	3.95 ± 0.29^b	6.46 ± 1.02^c	4.58 ± 0.48^b	6.18 ± 1.76^c
Immunosuppresion	1.33 ± 0.03^a	2.50 ± 0.10^b	3.32 ± 0.29^b	3.83 ± 0.35^b	5.23 ± 1.33^c
Elastosis	1.05 ± 0.00^a	1.14 ± 0.01 ^{b}	1.23 ± 0.03 ^{c}	1.33 ± 0.02 ^{d}	1.48 ± 0.05 ^{e}
Singlet oxygen formation	1.03 ± 0.00^a	1.03 ± 0.0 ^{a}	1.07 ± 0.02 ^{a}	1.22 ± 0.03 ^{b}	1.38 ± 0.05 ^{c}
Photoaging	1.03 ± 0.00^a	1.03 ± 0.00 ^{a}	1.07 ± 0.02 ^{b}	1.19 ± 0.02 ^{c}	1.34 ± 0.05 ^{d}
SPF / UVAPF	1.19	2.15	2.93	2.56	2.96
λ_c	322	314	317	331	338

Table 3
Half maximal effective concentration (EC_{50}) and selective index (SI) for **1** and **2** on the different cell lines: 1064sK (human gingival fibroblasts), HACAT (human epidermal keratinocyte), HCT-116 (human colon cancer), H-460 (human lung cancer) and G-361 (human melanoma). n.d. = not detected. Values are expressed as mean ± standard deviation (SD) ($n = 3$). No significant differences were observed among cell lines in each compound (ANOVA,CI: 95 %, $p > 0.05$, table SM.1).

Compounds	Cell line	EC_{50} (mg mL^{-1})	SI by 1064sK	SI by HACAT
	1064sK	8.00 ± 3.57	–	–
	HACAT	3.06 ± 1.81	–	–
1	HCT-116	5.35 ± 2.88	1.49	0.57
	H-460	7.76 ± 3.12	1.03	0.40
	G-361	9.48 ± 2.04	0.84	0.32
	1064sK	n.d.	–	–
	HACAT	4.96 ± 3.30	–	–
2	HCT-116	11.32 ± 8.36	–	0.44
	H-460	11.43 ± 4.00	–	0.43
	G-361	n.d.	–	–

calculated for compound **1** were obtained when comparing the three tumoral cell lines to 1064sK (HCT-116, > 3.96; H-460, > 1.03; and G-361, > 0.84) (Table 3). These were in most cases higher than the SI values calculated by comparison to HACAT or for compound **2,** all ranging between 0.32 and 1.63. In conclusion, compound **2** is less toxic than **1**, which on the other hand showed a more selective antitumoral activity against HCT-116 cells (SI: 1.49). The *Z*-factors for the MTT assay in all cell lines were: 1064sK: 0.65, HACAT: 0.75, HCT-116: 0.78, H-460: 0.90 and G-361: 0.85.

Toxicity of both synthetic compounds was also determined by using a zebrafish embryo toxicity assay to test concentration ranges below 20 mg mL^{-1} in three replicates. Although low, toxicity of compound **2** on zebrafish embryos was slightly higher than that of compound **1**. By using the log-linear method [62], we were unable to calculate a LC_{50} for any of both compounds in either 48 (Z factor = 1) or 72 (Z factor = 0.48) hpf larvae. Nevertheless, whereas compound **1**-treated 72 hpf larvae showed almost 100 % viability at the highest concentration, two replicates of compound **2** showed 82 % ($n = 11$) and 50 % ($n = 12$) viabilities at this time period. Although accuracy at 72 hpf is only sufficient (Z factor slightly lower than 0.5), these results suggest very low toxicity of both compounds.

Other possible signs of embryo toxicity were searched under the magnifying microscope after 48 or 72 h of treatments. Whereas compound **1** showed no teratogenic effect, compound **2** showed hatching delay at 48 hpf and sporadic heart oedema and dysplasia at 72 hpf. These toxic effects did not show any statistical relationship with concentration. Nevertheless, the hatching percentage of 48 hpf embryos showed a slight reduction trend as compound **2** concentration increased (Fig. 5, Z factor = 1). Although the accuracy of the method is high at this point (Z factor higher than 0.5), the reduction showed no significance either (Kruskal-Wallis test, $p > 0.05$).

In general, our results suggest absence of toxicity over zebrafish larvae development of compound **1** at concentrations below 20 mg mL^{-1}. In the case of compound **2**, some slight, statistically non-significant toxic effects have been observed when incubated in concentrations over 5 mg mL^{-1}.

4. Discussion

The development of a new group of synthetic UV-screen compounds inspired in the natural mycosporine-like amino acids (MAAs) opens new perspectives to the diversification of the UV filters currently available on the market [37]. The in-house preparation of these compounds is very convenient, *i.e.* the synthetic route is fast, cheap and quantitative. In addition, the characterization information obtained is in full agreement with reported data [65]. It should be noted that the photoprotection mechanism of these compounds is completely different from those of commercial synthetic UV filters, which usually involve a double bond isomerization (cinnamates) or an excited state proton transfer (avobenzone and oxybenzone) [66]. In the case of MAAs and related compounds, the photoprotection mechanism involves an out-of-plane distortion of the ring that leads to a very efficient energy dissipation of the excited state [38,39,67]. The lack of excited state minima could make these synthetic compounds safer for human health and the environment. In a different way, Osborn and Mahmud [68] have also developed a novel UV-screen compound known as Gadusporine, with a maximum absorption at 340 nm. This compound has been obtained by mixing and matching MAAs and gadusol biosynthetic genes from one vertebrate and two Gram (−) bacteria. Interestingly, natural MAAs are thought to have both UV-screen and antioxidant properties that would allow them to protect living organisms from the deleterious effects of light and ROS.

The antioxidant capacity of MAAs have been analyzed by different authors *in vitro* [30,32,36]. Using different methods, de la Coba et al. and

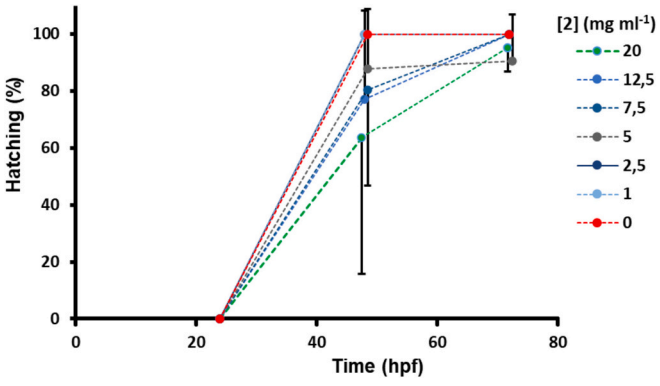

Fig. 5. Temporal variations of hatching percentage of 48 hpf zebrafish larvae treated with increasing concentrations of compound **2.** Values are means and vertical bars SD from three independent replicas ($n > 30$). (B). Colour code at the right are concentrations of compound **2** in mg mL^{-1}. No statistical significance is found between any pair of concentration groups (Kruskal-Wallis test, CI: 95 %, $p > 0.05$) and the pairwise comparisons (Bonferroni procedure, CI: 95 %, $p > 0.05$ for each pair).

Torres et al. [30,32] evaluated the antioxidant potential of five MAAs (mycosporine-glycine, palythine, asterine-330, shinorine, and porphyra-334). In general, both authors agree that the antioxidant activity of all MAAs depends on the concentration and pH, with greater activity in an alkaline environment (8.5). By using the ABTS radical scavenging assay, de la Coba et al. [30] observed the highest antioxidant capacity (83 %) in the oxo-MAA mycosporine-glycine at 10 μM and pH 8.5. Other MAAs, such as asterina-330 or porphyra-334 showed a 47 % and 15 % of antioxidant capacity, respectively. At higher pH (10.5), MAAs were degraded [31]. The synthetic compounds analyzed in our study are more like the oxo-MAAs, which have a single nitrogen substituent in the C3 of the cyclohexanone ring, than the imino-MAAs, which have two nitrogen substituents in C1 and C3 of the cyclohexenimine ring. The comparison of our results with other natural isolated MAAs is also difficult due to the different methodologies and units used. However, the antioxidant values obtained from compounds **1** and **2** were high compared to those obtained from algae extracts with MAAs (about 15–20 μmol TE g^{-1} DW in *Porphyra sp.*) [69,70]. Although these studies conclude that MAAs can eliminate ROS *in vitro*, their role *in vivo* is not yet fully understood [36].

In relation to photoprotection, de la Coba et al. [31] analyzed different cosmetic formulations with isolated MAAs that reached SPF values of 6.5 when 5 % of Myc-serinol was added. Among the different formulations with compounds **1** and **2** tested in our study, both with similar maximum absorptions (λ_{max}: 310, 290 and 300 nm), only 5 % of compound **2** showed comparable SPF or UVAPF (4 and 1.4, respectively). De la Coba et al. [31] achieved an even higher SPF (8.4) combining two types of MAAs: Myc-serinol (λ_{max}: 310 nm) and Porphyra-334 (λ_{max}: 334 nm). Indeed, commercial formulations of sunscreens contain a combination of different UV filters in order to cover the complete UV spectrum and achieve a higher photoprotection. In this sense, our compounds could also be combined with other MAAs from the same family [37]. Examples of this are the natural MAAs Myc-glycine, with λ_{max} at 310 nm, and Porphyra-334, with λ_{max} at 334 nm, or other natural compounds, such as phenolic compounds, carotenoids or scytonemin. In a previous report, Losantos et al. [37] measured SPF and UVAPF values of molecules of a similar synthetic nature. A cosmetic formulation with two synthetic compounds (10 % each one), one with λ_{max} at 306 nm and the other at 328 nm, showed a SPF of 6 and a UVAPF of 4.5. Interestingly, when these compounds were combined with octinoxate and avobenzone, a clear booster effect were observed. In this case, the SPF increased from 29 (only commercial synthetic UV filters) to 73, and the UVAPF from 12 to 23. Recently, this family of compounds have been tested as stabilizer of avobenzone, a widely used UVA filter in cosmetic products. Some of these compounds were able to increase the UV required for avobenzone photobleaching, although they were not able to enhance octocrylene photoprotection [71]. As the natural MAAs, these new compounds may show other beneficial effects on skin health that would merit further investigations.

In contrast to the relatively low SPF values observed, our compounds showed a great photostability at the concentration used. Even after a UV radiation dose of 167.2 kJ m^{-2}, the SPF and UVAPF values did not decrease suggesting that the molecules were not degraded. The highest UV radiation dose used for photostability correspond to 2.5–4 MEDs (Table 1). The MED is defined as the minimal UV dose required to produce a perceptible erythema in the skin. Depending on the skin phototype, the MED vary from 150 to 300 J m^{-2} in phototype I, to 900–1500 J m^{-2} in phototype VI. In a summer day, the sun exposure time required to produce the MED for a phototype II skin is 26–35 min [72]. Therefore, these compounds would remain stable during an appropriate UV exposure time, making them suitable for their inclusion in sunscreens. The stability was also observed by Losantos et al. [37] in similar synthetic molecules. This is reminiscent of the high photostability shown by the natural MAAs [73]. As some commercial synthetic UV filters are photodegraded by UV radiation into products with molecular instability and loss of efficiency [74], this family of compounds offers an advantageous alternative. Finally, the versality of these compounds offers different alternatives of incorporation into the cosmetic formulations (*e.g.* encapsulation or pickering effect) providing further advantages.

Although the toxicity of this new family of molecules had not been tested yet, it has been postulated that they are non-toxic [71]. To our certain knowledge, this is the first study that determines *in vitro* and *in vivo* the toxicity of two members of this new molecular family. Regarding *in vitro* assays, the MTT methodology showed low toxicity of compounds **1** and **2** on healthy cell lines (1064sk or HACAT) but significant toxicity on cancer cells (HCT-116, H-460 or G-361). In this assay, the higher the half maximal effective concentration (EC_{50}), the lower the toxicity of the reagent evaluated.

Compound **1** showed an EC_{50} on 1064sk cells of 8.0 mg mL^{-1} in contrast with compound **2,** that does not affect the cell proliferation rates in a way that represents toxicity. In fact, compounds **1** and **2** showed similar values on HACAT cells (4.96 and 3.06 mg mL^{-1}, respectively). Searching for possible therapeutic applications, carcinogenic cells were also tested. In the MTT methodology, a selective index (SI) may also be obtained. The greater the SI value, the more selectivity is shown by the tested compound. According to Indrayanto et al. [58], compounds with SI values higher than 3 are potential anticancer drugs that should be further investigated. Compound **1** showed a low EC_{50} on HCT-116 cells (5.35 ± 2.88 mg mL^{-1}) and a selectivity index of 1.49, suggesting a relative anti-tumor activity against colon cancer. In contrast, compound **2** did not show toxicity in any cell line. In the studies cited above, natural MAAs have also shown non-toxicity on cell lines *in vitro*. Some of these compounds even show an enhancer effect of cellular proliferation and wound healing [27,75]. The synthetic UV screen compounds showed zero toxicity similar to natural MAAs [27] or other natural compounds extracted from algae, such as polysaccharides (*e.g.* Ulvans present a EC_{50} of 4.2 and 1.2 mg mL^{-1} on HACAT and 1064sk cells; [62]).

The zebrafish (*Danio rerio*) has been previously used to evaluate toxicity of some commercial UV filters. Blüthgen et al. [76] observed multiple hormonal activities at the transcription level under low concentration of oxybenzone in zebrafish. Similar results were also found by Downs et al. and Weisbrod et al. [13,77] when testing benzophenonoe-2 on zebrafish. Among a variety of toxicity assays found in the literature [78–83], we have chosen a variant of the zebrafish embryo acute toxicity (ZFET) test [74]previously published by other groups [59,84]. The low toxicity found following the *in vitro* assay was confirmed by the ZFET. This assay not only determines a median lethal concentration (LC_{50}) of the compound, but also studies teratogenic effects using an extensive phenotypic panel [83]. By applying the ZFET, neither a LC_{50} could be calculated for compounds **1** or **2** over 20 mg mL^{-1} nor statistical significance was found for the teratogenic effects. Only compound **2** showed a slight, non statistically significant effect over hatching, heart oedema or anatomical dysplasia [62,83,85–89], [90].

Among other teratogenic phenotypes, embryo depigmentation has been proposed to evaluate potential anticancer compounds interfering tyrosine kinase activities when high LC_{50} are calculated in zebrafish assays [91, 92]. In our study, no depigmentation was found, suggesting that the potential cytotoxic effects observed in cancer cell lines could be unrelated to tyrosine kinases [92].

In summary, no significant toxicity of compounds **1** and **2** have been found using the ZFET assay. This low or absent toxicity agrees with the sunscreen activity of gadusol, an endogenous microsporine-like molecules in zebrafish that it is expressed during development [93]. However, compound **1** emerges as a promising candidate for photoprotection filters, the slight toxicity effects observed in treatments with compound **2** concentrations over 5 mg mL^{-1} clearly restrict its potential therapeutic index. In any case, further toxicity studies should be performed in higher vertebrates (*i.e.* rodents) to stimulate the application of the compounds to humans.

5. Concluding remarks

Considering the low toxicity of compounds **1** and **2** (both, on cell lines and zebrafish embryos), these molecules could be potential alternatives to current commercial UV filters. They show relevant combined properties due to their antioxidant capacity and photostability to be used as additives in commercial formulations in place of compounds currently under safety scrutiny. However, their relatively low SPF values lead us to suggest that they should be combined with other compounds (natural or not) to increase the photoprotection capacity. Thus, this study should be extended to other members of the cyclohexanone family looking for improved properties and, eventually, to different chemical cores aiming for compounds with increased performance.

Bioethical approvals

Experiments were approved by the UMA Bioethics commission (ref. 100–2018-T).

CRediT authorship contribution statement

Félix L. Figueroa: Writing – review & editing, Writing – original draft, Supervision, Resources, Investigation, Funding acquisition, Conceptualization. **Pablo Castro-Varela:** Writing – review & editing, Writing – original draft, Methodology, Investigation, Formal analysis. **Julia Vega:** Writing – review & editing, Writing – original draft, Methodology, Investigation, Formal analysis. **Raúl Losantos:** Writing – review & editing, Methodology, Investigation, Formal analysis, Data curation. **Beatriz Peñín:** Writing – review & editing, Methodology, Investigation, Formal analysis, Data curation. **Leonardo López-Cóndor:** Writing – review & editing, Methodology, Investigation, Formal analysis, Data curation. **María Jesús Pacheco:** Writing – review & editing, Methodology, Investigation, Formal analysis, Data curation. **Sofía Latorre Redoli:** Investigation, Methodology, Resources, Writing – review & editing. **Manuel Marí-Beffa:** Writing – review & editing, Writing – original draft, Supervision, Resources, Methodology, Investigation, Formal analysis, Conceptualization. **Roberto Abdala-Díaz:** Writing – review & editing, Supervision, Resources, Investigation, Formal analysis. **Diego Sampedro:** Writing – review & editing, Writing – original draft, Supervision, Resources, Methodology, Investigation, Funding acquisition, Formal analysis, Conceptualization.

Declaration of competing interest

Authors declare no competing financial interests or personal relationships that may have influenced the elaboration of this article.

Acknowledgements

This study was funded by the Ministry of Science and Innovation (Spain) through the projects TED2021-131555B-C22, PDC2021-121410-I00 and PID2021-126075NB-I00 and the group BIO 217 (Andalusian Government and FEDER). MJP was recipient of a fellowship from UMA18-FEDERJA-274 grant. SLR was recipient of a A.1. grant from the University of Málaga (Plan Propio de Investigación y Transferencia). Authors are deeply indebted to Candela Caneda-Santiago and Piedad Valverde-Guillén for technical support. Microscopical studies were performed in the Microscopy Service of "Central Services of Research Support" of the UMA. "CIBER-BBN" is an initiative from the ISCIII of Spain. R.L. acknowledges Universidad de La Rioja for his contract on Sustainable development 004/2023. B.P. thanks Universidad de La Rioja for her fellowship. Funders have no role in the design or realization of this work.

Appendix A. Supplementary data

Supplementary data to this article can be found online at https://doi.org/10.1016/j.jphotobiol.2024.113050.

Data availability

Data will be made available on request.

References

[1] A.F. Bais, G. Bernhard, R.L. McKenzie, P.J. Aucamp, P.J. Young, M. Ilyas, P. Jöckel, M. Deushi, Ozone–climate interactions and effects on solar ultraviolet radiation, Photochem. Photobiol. Sci. 18 (2019) 602–640, https://doi.org/10.1039/C8PP90059K.

[2] R.E. Neale, P.W. Barnes, T.M. Robson, P.J. Neale, C.E. Williamson, R.G. Zepp, S. R. Wilson, S. Madronich, A.L. Andrady, A.M. Heikkilä, G.H. Bernhard, A.F. Bais, P. J. Aucamp, A.T. Banaszak, J.F. Bornman, L.S. Bruckman, S.N. Byrne, B. Foereid, D. P. Häder, L.M. Hollestein, W.C. Hou, S. Hylander, M.A.K. Jansen, A.R. Klekociuk, J. B. Liley, J. Longstreth, R.M. Lucas, J. Martinez-Abaigar, K. McNeill, C.M. Olsen, K. K. Pandey, L.E. Rhodes, S.A. Robinson, K.C. Rose, T. Schikowski, K.R. Solomon, B. Sulzberger, J.E. Ukpebor, Q.W. Wang, S. Wängberg, C.C. White, S. Yazar, A. R. Young, P.J. Young, L. Zhu, M. Zhu, Environmental effects of stratospheric ozone depletion, UV radiation, and interactions with climate change: UNEP environmental effects assessment panel, update 2020, Photochem. Photobiol. Sci. 20 (2021) 1–67, https://doi.org/10.1007/S43630-020-00001-X.

[3] G. Williamson, C.D. Kay, A. Crozier, The bioavailability. Transport, and bioactivity of dietary flavonoids: a review from a historical perspective, Compr. Rev. Food Sci. Food Saf. 17 (2018) 1054–1112, https://doi.org/10.1111/1541-4337.12351.

[4] I.V. Ivanov, T. Mappes, P. Schaupp, C. Lappe, S. Wahl, Ultraviolet radiation oxidative stress affects eye health, J. Biophotonics 11 (2018) e201700377, https://doi.org/10.1002/JBIO.201700377.

[5] R.M. Lucas, S. Yazar, A.R. Young, M. Norval, F.R. De Gruijl, Y. Takizawa, L. E. Rhodes, C.A. Sinclair, R.E. Neale, Human health in relation to exposure to solar ultraviolet radiation under changing stratospheric ozone and climate, Photochem. Photobiol. Sci. 18 (2019) 641–680, https://doi.org/10.1039/C8PP90060D.

[6] P. Thomas, A. Swaminathan, R.M. Lucas, Climate change and health with an emphasis on interactions with ultraviolet radiation: a review, Glob. Chang. Biol. 18 (2012) 2392–2405, https://doi.org/10.1111/J.1365-2486.2012.02706.X.

[7] J. D'Orazio, S. Jarrett, A. Amaro-Ortiz, T. Scott, UV radiation and the skin, Int. J. Mol. Sci. 14 (2013) 12222–12248, https://doi.org/10.3390/IJMS140612222.

[8] S. González, M. Fernández-Lorente, Y. Gilaberte-Calzada, The latest on skin photoprotection, Clin. Dermatol. 26 (2008) 614–626, https://doi.org/10.1016/J.CLINDERMATOL.2007.09.010.

[9] M. Sander, M. Sander, T. Burbidge, J. Beecker, The efficacy and safety of sunscreen use for the prevention of skin cancer, CMAJ 192 (2020) E1802–E1808, https://doi.org/10.1503/CMAJ.201085/TAB-RELATED-CONTENT.

[10] L. Vidal-Liñán, E. Villaverde-de-Sáa, R. Rodil, J.B. Quintana, R. Beiras, Bioaccumulation of UV filters in *Mytilus galloprovincialis* mussel, Chemosphere 190 (2018) 267–271, https://doi.org/10.1016/J.CHEMOSPHERE.2017.09.144.

[11] V. Prakash, S. Anbumani, A systematic review on occurrence and ecotoxicity of organic UV filters in aquatic organisms, Rev. Environ. Contam. Toxicol. 257 (2021) 121–161, https://doi.org/10.1007/398_2021_68/TABLES/1.

[12] M.J. Araújo, R.J.M. Rocha, A.M.V.M. Soares, J.L. Benedé, A. Chisvert, M. S. Monteiro, Effects of UV filter 4-methylbenzylidene camphor during early development of *Solea senegalensis* Kaup, Sci. Total Environ. 628–629 (2018) (1858) 1395–1404, https://doi.org/10.1016/J.SCITOTENV.2018.02.112.

[13] C.A. Downs, E. Kramarsky-Winter, R. Segal, J. Fauth, S. Knutson, O. Bronstein, F. R. Ciner, R. Jeger, Y. Lichtenfeld, C.M. Woodley, P. Pennington, K. Cadenas, A. Kushmaro, Y. Loya, Toxicopathological effects of the sunscreen UV Filter, oxybenzone (benzophenone-3), on coral planulae and cultured primary cells and its environmental contamination in Hawaii and the U.S. Virgin Islands, Arch. Environ. Contam. Toxicol. 70 (2016) 265–288, https://doi.org/10.1007/s00244-015-0227-7.

[14] B. Nataraj, K. Maharajan, D. Hemalatha, B. Rangasamy, N. Arul, M. Ramesh, Comparative toxicity of UV-filter Octyl methoxycinnamate and its photoproducts on zebrafish development, Sci. Total Environ. 718 (2020) 134546, https://doi.org/10.1016/J.SCITOTENV.2019.134546.

[15] E. Thorel, F. Clergeaud, L. Jaugeon, A.M.S. Rodrigues, J. Lucas, D. Stien, P. Lebaron, Effect of 10 UV filters on the brine shrimp *Artemia salina* and the marine microalga *Tetraselmis* sp. Toxics 29 (2020) https://doi.org/10.3390/TOXICS8020029.

[16] M.M.P. Tsui, J.C.W. Lam, T.Y. Ng, P.O. Ang, M.B. Murphy, P.K.S. Lam, Occurrence, distribution, and fate of organic UV filters in coral communities, Environ. Sci. Technol. 51 (2017) 4182–4190, https://doi.org/10.1021/acs.est.6b05211.

[17] D. Vuckovic, A.I. Tinoco, L. Ling, C. Renicke, J.R. Pringle, W.A. Mitch, Conversion of oxybenzone sunscreen to phototoxic glucoside conjugates by sea anemones and corals, Science 376 (2022), https://doi.org/10.1126/SCIENCE.ABN2600/SUPPL_FILE/SCIENCE.ABN2600_DATA_S1_TO_S10.ZIP.

[18] S. Santander Ballestín, M.J. Luesma Bartolomé, Toxicity of different chemical components in sun cream filters and their impact on human health: a review, Appl. Sci. (2023) 712, https://doi.org/10.3390/APP13020712.

[19] J. Wang, L. Pan, S. Wu, L. Lu, Y. Xu, Y. Zhu, M. Guo, S. Zhuang, Recent advances on endocrine disrupting effects of UV filters, Int. J. Environ. Res. Public Health (2016) 782, https://doi.org/10.3390/IJERPH13080782.

[20] EC, Regulation (EC) No 1223/2009 of the European Parliament and of the Council of 30 November 2009 on Cosmetic Products, 2009.

[21] FDA, 21 C.F.R. 352 - Sunscreen Drug Products for Over-the-Counter Human Use, 2004.

[22] EC, Commission Regulation (EU) 2022/1176, Amending Regulation (EC) No 1223/2009 as Regards the Use of Certain UV Filters in Cosmetic Products, 2022.

[23] A. Levine, Reducing the prevalence of chemical UV filters from sunscreen in aquatic environments: regulatory, public awareness, and other considerations, Integr. Environ. Assess. Manag. 17 (2021) 982–988, https://doi.org/10.1002/IEAM.4432.

[24] J.I. Carreto, M.O. Carignan, Mycosporine-like amino acids: relevant secondary metabolites. Chemical and ecological aspects, Mar. Drugs 9 (2011) 387–446, https://doi.org/10.3390/md9030387.

[25] E. Chrapusta, A. Kaminski, K. Duchnik, B. Bober, M. Adamski, J. Bialczyk, Mycosporine-like amino acids: potential health and beauty ingredients, Mar. Drugs 15 (2017) 326, https://doi.org/10.3390/md15100326.

[26] J. Vega, G. Schneider, B.R. Moreira, C. Herrera, J. Bonomi-Barufi, F.L. Figueroa, Mycosporine-like amino acids from red macroalgae: UV-photoprotectors with potential cosmeceutical applications, Appl. Sci. 11 (2021) 5112, https://doi.org/10.3390/APP11115112.

[27] K.P. Lawrence, P.F. Long, A.R. Young, Mycosporine-like amino acids for skin photoprotection, Curr. Med. Chem. 25 (2017) 5512–5527, https://doi.org/10.2174/0929867324666170529124237.

[28] N. Rosic, M. Climstein, G.M. Boyle, D. Thanh Nguyen, Y. Feng, Exploring Mycosporine-like amino acid UV-absorbing natural products for a new generation of environmentally friendly sunscreens, Mar. Drugs 21 (2023) 253, https://doi.org/10.3390/MD21040253.

[29] D. Sampedro, Computational exploration of natural sunscreens, Phys. Chem. Chem. Phys. 13 (2011) 5584–5586, https://doi.org/10.1039/C0CP02901G.

[30] F. de la Coba, J. Aguilera, F.L. Figueroa, M.V. de Gálvez, E. Herrera, Antioxidant activity of mycosporine-like amino acids isolated from three red macroalgae and one marine lichen, J. Appl. Phycol. 21 (2009) 161–169, https://doi.org/10.1007/s10811-008-9345-1.

[31] F. de la Coba, J. Aguilera, N. Korbee, M.V. de Gálvez, E. Herrera-Ceballos, F. Álvarez-Gómez, F.L. Figueroa, UVA and UVB Photoprotective capabilities of topical formulations containing mycosporine-like amino acids (maas) through different biological effective protection factors (BEPFs), Mar. Drugs 17 (2019), https://doi.org/10.3390/md17010055.

[32] P. Torres, J.P. Santos, F. Chow, M.J. Pena Ferreira, D.Y.A.C. dos Santos, Comparative analysis of in vitro antioxidant capacities of mycosporine-like amino acids (MAAs), Algal Res. 34 (2018) 57–67, https://doi.org/10.1016/J.ALGAL.2018.07.007.

[33] A. Hartmann, J. Gostner, J.E. Fuchs, E. Chaita, N. Aligiannis, L. Skaltsounis, M. Ganzera, Inhibition of collagenase by mycosporine-like amino acids from marine sources, Planta Med. 81 (2015) 813–820, https://doi.org/10.1055/s-0035-1546105.

[34] K.P. Lawrence, R. Gacesa, P.F. Long, A.R. Young, Molecular photoprotection of human keratinocytes in vitro by the naturally occurring mycosporine-like amino acid palythine, Br. J. Dermatol. 178 (2018) 1353–1363, https://doi.org/10.1111/bjd.16125.

[35] K. Becker, A. Hartmann, M. Ganzera, D. Fuchs, J. Gostner, Immunomodulatory effects of the mycosporine-like amino acids shinorine and porphyra-334, Mar. Drugs 14 (2016) 119, https://doi.org/10.3390/md14060119.

[36] N. Wada, T. Sakamoto, S. Matsugo, Mycosporine-like amino acids and their derivatives as natural antioxidants, Antioxidants 4 (2015) 603–646, https://doi.org/10.3390/antiox4030603.

[37] R. Losantos, I. Funes-Ardoiz, J. Aguilera, E. Herrera-Ceballos, C. García-Iriepa, P. J. Campos, D. Sampedro, Rational design and synthesis of efficient sunscreens to boost the solar protection factor, Angew. Chem. 129 (2017) 2676–2679, https://doi.org/10.1002/ANGE.201611627.

[38] A.M. Cowden, R. Losantos, A.L. Whittock, B. Peñín, D. Sampedro, V.G. Stavros, Ring buckling and C=N isomerization pathways for efficient photoprotection in two nature-inspired UVA sunscreens revealed through ultrafast dynamics and high-level calculations, Photochem. Photobiol. 00 (2023) 1–16, https://doi.org/10.1111/PHP.13823.

[39] R. Losantos, I. Lamas, R. Montero, A. Longarte, D. Sampedro, Photophysical characterization of new and efficient synthetic sunscreens, Phys. Chem. Chem. Phys. 21 (2019) 11376–11384, https://doi.org/10.1039/C9CP01267B.

[40] A.D. Becke, Density-functional thermochemistry. III. The role of exact exchange, J. Chem. Phys. 98 (1993) 5648–5652, https://doi.org/10.1063/1.464913.

[41] R. Ditchfield, W.J. Hehre, J.A. Pople, Self-consistent molecular-orbital methods. IX. An extended Gaussian-type basis for molecular-orbital studies of organic molecules, J. Chem. Phys. 54 (1971) 724–728, https://doi.org/10.1063/1.1674902.

[42] G. Scalmani, M.J. Frisch, Continuous surface charge polarizable continuum models of solvation. I. General formalism, J. Chem. Phys. 132 (2010), https://doi.org/10.1063/1.3359469/939624.

[43] F. Trani, G. Scalmani, G. Zheng, I. Carnimeo, M.J. Frisch, V. Barone, Time-dependent density functional tight binding: new formulation and benchmark of excited states, J. Chem. Theory Comput. 7 (2011) 3304–3313, https://doi.org/10.1021/CT200461Y/SUPPL_FILE/CT200461Y_SI_001.PDF.

[44] R.L. Martin, Natural transition orbitals, J. Chem. Phys. 118 (2003) 4775–4777, https://doi.org/10.1063/1.1558471.

[45] M.J. Frisch, G.W. Trucks, H.B. Schlegel, G.E. Scuseria, M.A. Robb, J.R. Cheeseman, G. Scalmani, V. Barone, G.A. Petersson, H. Nakatsuji, X. Li, M. Caricato, A. V. Marenich, J. Bloino, B.G. Janesko, R. Gomperts, B. Mennucci, H.P. Hratchian, GAUSSIAN, Gaussian, Inc, Wallingford, 2016.

[46] R. Re, N. Pellegrini, A. Proteggente, A. Pannala, M. Yang, C. Rice-Evans, Antioxidant activity applying an improved ABTS radical cation decolorization assay, Free Radic. Biol. Med. 26 (1999) 1231–1237, https://doi.org/10.1016/S0891-5849(98)00315-3.

[47] W. Brand-Williams, M.E. Cuvelier, C. Berset, Use of a free radical method to evaluate antioxidant activity, LWT Food Sci. Technol. 28 (1995) 25–30, https://doi.org/10.1016/S0023-6438(95)80008-5.

[48] M. Pissavini, C. Tricaud, G. Wiener, A. Lauer, M. Contier, L. Kolbe, C. Trullás Cabanas, F. Boyer, V. Nollent, E. Meredith, E. Dietrich, P.J. Matts, Validation of an in vitro sun protection factor (SPF) method in blinded ring-testing, Int. J. Cosmet. Sci. 40 (2018) 263–268, https://doi.org/10.1111/ics.12459.

[49] ISO 24443, Determination of Sunscreen UVA Photoprotection In Vitro. https://www.iso.org/standard/46522.html, 2012 accessed August 25, 2023.

[50] A.F. McKinlay, Reference action spectrum for ultraviolet induced erythema in human skin, CIE-Journal 6 (1987) 17–22. https://ci.nii.ac.jp/naid/10014528135/. accessed October 12, 2020.

[51] D. Moyal, A. Chardon, N. Kollias, UVA protection efficacy of sunscreens can be determined by thepersistent pigment darkening (PPD) method, Photodermatol. Photoimmunol. Photomed. 16 (2000) 250–255, https://doi.org/10.1034/J.1600-0781.2000.160603.X.

[52] F.R. de Gruijl, J.C. Van der Leun, Estimate of the wavelength dependency of ultraviolet carcinogenesis in humans and its relevance to the risk assessment of a stratospheric ozone depletion, Health Phys. 67 (1994) 319–325.

[53] E.C.D. Fabo, M.L. Kripke, Wavelength dependence and dose-rate independence of UV radiation-induced immunologic unresponsiveness of mice to a UV-induced fibrosarcoma, Photochem. Photobiol. 32 (1980) 183–188, https://doi.org/10.1111/j.1751-1097.1980.tb04007.x.

[54] H.C. Wulf, T. Poulsen, R.E. Davies, F. Urbach, Narrow-band UV radiation and induction of dermal elastosis and skin cancer, Photodermatol 6 (1989) 44–51.

[55] K.M. Hanson, J.D. Simon, Epidermal trans-urocanic acid and the UV-A-induced photoaging of the skin, Proc. Natl. Acad. Sci. 95 (1998) 10576–10578, https://doi.org/10.1073/PNAS.95.18.10576.

[56] D.L. Bissett, D.P. Hannon, T.V. Orr, Wavelength dependence of histological, physical and visible changes in chronically UV-irradiated hairless mouse skin, Photochem. Photobiol. 50 (1989) 763–769, https://doi.org/10.1111/j.1751-1097.1989.tb02907.x.

[57] P. Castro-Varela, M. Rubilar, B. Rodrigues, M.J. Pacheco, C.T. Caneda-Santiago, M. Marí-Beffa, F.L. Figueroa, R. Abdala-Díaz, A sequential recovery extraction and biological activity of water-soluble sulfated polysaccharides from the polar red macroalgae *Sarcopeltis skottsbergii*, Algal Res. 73 (2023) 103160, https://doi.org/10.1016/J.ALGAL.2023.103160.

[58] G. Indrayanto, G.S. Putra, F. Suhud, Validation of in-vitro bioassay methods: application in herbal drug research, Profiles Drug Subst. Excip. Relat. Methodol. 46 (2021) 273–307, https://doi.org/10.1016/BS.PODRM.2020.07.005.

[59] S.R.A. Usuldin, W.A.A.Q.I. Wan-Mohtar, Z. Ilham, A.A. Jamaludin, N.R. Abdullah, N. Rowan, In vivo toxicity of bioreactor-grown biomass and exopolysaccharides from Malaysian tiger milk mushroom mycelium for potential future health applications, Sci. Rep. 11 (2021) 1–13, https://doi.org/10.1038/s41598-021-02486-7.

[60] M. Westerfield, The Zebrafish Book: A Guide for the Laboratory Use of Zebrafish (*Danio rerio*), Univ. of Oregon Press, Eugene, 1995, https://doi.org/10.1371/JOURNAL.PGEN.1005483.

[61] J. García-Márquez, B.R. Moreira, P. Valverde-Guillén, S. Latorre-Redoli, C. T. Caneda-Santiago, G. Acién, E. Martínez-Manzanares, M. Marí-Beffa, R.T. Abdala-Díaz, In vitro and in vivo effects of Ulvan polysaccharides from *Ulva rigida*, Pharmaceuticals 16 (2023) 660, https://doi.org/10.3390/PH16050660.

[62] M.C. Ocaña, B. Martínez-Poveda, M. Marí-Beffa, A.R. Quesada, M.Á. Medina, Fasentin diminishes endothelial cell proliferation, differentiation and invasion in a glucose metabolism-independent manner, Sci. Rep. 10 (2020) 1–14, https://doi.org/10.1038/s41598-020-63232-z.

[63] A. Cantrell, D.J. McGarvey, Photochemical studies of 4-tert-butyl-4′-methoxydibenzoylmethane (BM-DBM), J. Photochem. Photobiol. B 64 (2001) 117–122, https://doi.org/10.1016/S1011-1344(01)00226-3.

[64] J.M. Woolley, R. Losantos, D. Sampedro, V.G. Stavros, Computational and experimental characterization of novel ultraviolet filters, Phys. Chem. Chem. Phys. 22 (2020) 25390–25395, https://doi.org/10.1039/D0CP04940A.

[65] A.R. Osborn, T. Mahmud, Interkingdom genetic mix-and-match to produce novel sunscreens, ACS Synth. Biol. 8 (2019) 2464–2471, https://doi.org/10.1021/ACSSYNBIO.9B00352/ASSET/IMAGES/LARGE/SB9B00352_0005.JPEG.

[66] G. Schneider, F.L. Figueroa, J. Vega, P. Chaves, F. Álvarez-Gómez, N. Korbee, J. Bonomi-Barufi, Photoprotection properties of marine photosynthetic organisms grown in high ultraviolet exposure areas: cosmeceutical applications, Algal Res. 49 (2020) 101956, https://doi.org/10.1016/j.algal.2020.101956.

[67] J. Vega, J. Bonomi-Barufi, J.L. Gómez-Pinchetti, F.L. Figueroa, Cyanobacteria and red macroalgae as potential sources of antioxidants and UV radiation-absorbing compounds for cosmeceutical applications, Mar. Drugs 18 (2020) 659, https://doi.org/10.3390/md18120659.

[68] J. Soilán, L. López-Cóndor, B. Peñín, J. Aguilera, M. Victoria De Gálvez, D. Sampedro, R. Losantos, Evaluation of MAA analogues as potential candidates to increase photostability in sunscreen formulations, Photochem 4 (2024) 128–137, https://doi.org/10.3390/PHOTOCHEM4010007.

[69] F.R. Conde, M.S. Churio, C.M. Previtali, Experimental study of the excited-state properties and photostability of the mycosporine-like amino acid palythine in aqueous solution, Photochem. Photobiol. Sci. 6 (2007) 669–674, https://doi.org/10.1039/B618314J.
[70] J. Kockler, M. Oelgemöller, S. Robertson, B.D. Glass, Photostability of sunscreens, J. Photochem. Photobiol. C Photchem. Rev. 13 (2012) 91–110, https://doi.org/10.1016/j.jphotochemrev.2011.12.001.
[71] M. Orfanoudaki, A. Hartmann, M. Alilou, T. Gelbrich, P. Planchenault, S. Derbré, A. Schinkovitz, P. Richomme, A. Hensel, M. Ganzera, Absolute configuration of mycosporine-like amino acids, their wound healing properties and in vitro anti-aging effects, Mar. Drugs 18 (2019) 35, https://doi.org/10.3390/md18010035.
[72] N. Blüthgen, S. Zucchi, K. Fent, Effects of the UV filter benzophenone-3 (oxybenzone) at low concentrations in zebrafish (*Danio rerio*), Toxicol. Appl. Pharmacol. 263 (2012) 184–194, https://doi.org/10.1016/j.taap.2012.06.008.
[73] C.J. Weisbrod, P.Y. Kunz, A.K. Zenker, K. Fent, Effects of the UV filter benzophenone-2 on reproduction in fish, Toxicol. Appl. Pharmacol. 225 (2007) 255–266, https://doi.org/10.1016/j.taap.2007.08.004.
[74] J.C. Achenbach, C. Leggiadro, S.A. Sperker, C. Woodland, L.D. Ellis, Comparison of the zebrafish embryo toxicity assay and the general and behavioral embryo toxicity assay as new approach methods for chemical screening, Toxics 8 (2020) 126, https://doi.org/10.3390/TOXICS8040126.
[75] ISO 15088:2007(en), Water Quality — Determination of the Acute Toxicity of Waste Water to Zebrafish Eggs (*Danio rerio*). https://www.iso.org/obp/ui/en/#iso:std:iso:15088:ed-1:v1:en, 2024 accessed June 29, 2024.
[76] A.L. Gustafson, D.B. Stedman, J. Ball, J.M. Hillegass, A. Flood, C.X. Zhang, J. Panzica-Kelly, J. Cao, A. Coburn, B.P. Enright, M.B. Tornesi, M. Hetheridge, K. A. Augustine-Rauch, Inter-laboratory assessment of a harmonized zebrafish developmental toxicology assay – Progress report on phase I, Reprod. Toxicol. 33 (2012) 155–164, https://doi.org/10.1016/J.REPROTOX.2011.12.004.
[77] A. Alzualde, M. Behl, N.S. Sipes, J.H. Hsieh, A. Alday, R.R. Tice, R.S. Paules, A. Muriana, C. Quevedo, Toxicity profiling of flame retardants in zebrafish embryos using a battery of assays for developmental toxicity, neurotoxicity, cardiotoxicity and hepatotoxicity toward human relevance, Neurotoxicol. Teratol. 70 (2018) 40–50, https://doi.org/10.1016/J.NTT.2018.10.002.
[78] S. Weigt, N. Huebler, R. Strecker, T. Braunbeck, T.H. Broschard, Zebrafish (Danio rerio) embryos as a model for testing proteratogens, Toxicology 281 (2011) 25–36, https://doi.org/10.1016/J.TOX.2011.01.004.
[79] L. Truong, R.L. Tanguay, Evaluation of embryotoxicity using the zebrafish model, Methods Mol. Biol. 1641 (2017) 325–333, https://doi.org/10.1007/978-1-4939-7172-5_18/FIGURES/2.
[80] A. Muthuraman, M. Ramesh, F. Mustaffa, A. Nadeem, S. Nishat, N. Paramakrishnan, K.G. Lim, In silico and in vitro methods in the characterization of beta-carotene as pharmaceutical material via acetylcholine esterase inhibitory actions, Molecules 28 (2023) 4358, https://doi.org/10.3390/MOLECULES28114358.
[81] I.V. Nechaev, D.S. Pavlov, The species specificity of hatching enzyme and its effect on the duration of embryogenesis in the fish *Cichlasoma nigrofasciatum* (Cichlidae), Dokl. Biol. Sci. 394 (2004) 78–81, https://doi.org/10.1023/B:DOBS.0000017136.04664.66/METRICS.
[82] J. Ord, Ionic stress prompts premature hatching of zebrafish (*Danio rerio*) embryos, Fishes 4 (2019) 20, https://doi.org/10.3390/FISHES4010020.
[83] L.B. Romero-Sánchez, M. Marí-Beffa, P. Carrillo, M.Á. Medina, A. Díaz-Cuenca, Copper-containing mesoporous bioactive glass promotes angiogenesis in an in vivo zebrafish model, Acta Biomater. 68 (2018) 272–285, https://doi.org/10.1016/J.ACTBIO.2017.12.032.
[84] K. Vega-Granados, J. Cruz-Reyes, J.F. Horta-Marrón, M. Marí-Beffa, L. Díaz-Rubio, I. Córdova-Guerrero, D. Chávez-Velasco, M.C. Ocaña, M.A. Medina, L.B. Romero-Sánchez, Synthesis, characterization and biological evaluation of octyltrimethylammonium tetrathiotungstate, BioMetals 34 (2021) 107–117, https://doi.org/10.1007/S10534-020-00267-9/FIGURES/9.
[85] S. Lin, Y. Zhao, Z. Ji, J. Ear, C. Hyun Chang, H. Zhang, C. Low-Kam, K. Yamada, H. Meng, X. Wang, R. Liu, S. Pokhrel, L. Mädler, R. Damoiseaux, T. Xia, H. A. Godwin, S. Lin, A.E. Nel, S. Lin, Z. Ji, C.H. Chang, H. Zhang, H. Meng, X. Wang, R. Liu, T. Xia, H.A. Godwin, A.E. Nel, Y. Zhao, J. Ear, C. Low-Kam, K. Yamada, R. Damoiseaux, S. Pokhrel, L. Mädler, Zebrafish high-throughput screening to study the impact of dissolvable metal oxide nanoparticles on the hatching enzyme, ZHE1, Small 9 (2013) 1776–1785, https://doi.org/10.1002/SMLL.201202128.
[86] T. Varnali, M. Bozoflu, H. Şengönül, S.I. Kurt, Potential metal chelating ability of mycosporine-like amino acids: a computational research, Chem. Pap. 76 (2022) 2279–2291, https://doi.org/10.1007/S11696-021-02014-X/FIGURES/7.
[87] S. Colanesi, K.L. Taylor, N.D. Temperley, P.R. Lundegaard, D. Liu, T.E. North, H. Ishizaki, R.N. Kelsh, E.E. Patton, Small molecule screening identifies targetable zebrafish pigmentation pathways, Pigm. Cell Melanoma Res. 25 (2012) 131–143, https://doi.org/10.1111/J.1755-148X.2012.00977.X.
[88] N.A. Rusdi, C.S. Kue, K.X. Yu, B.F. Lau, L.Y. Chung, L.V. Kiew, Assessment of potential anticancer activity of brown seaweed compounds using zebrafish phenotypic assay, Nat. Prod. Commun. 14 (2019), https://doi.org/10.1177/1934578X19857909/ASSET/IMAGES/LARGE/10.1177_1934578X19857909-FIG5.JPEG.
[89] A.R. Osborn, K.H. Almabruk, G. Holzwarth, S. Asamizu, J. LaDu, K.M. Kean, P. A. Karplus, R.L. Tanguay, A.T. Bakalinsky, T. Mahmud, De novo synthesis of a sunscreen compound in vertebrates, Elife 4 (2015), https://doi.org/10.7554/ELIFE.05919.